light resetting pathway becomes functional or, alternatively, that an oscillating clock cannot be entirely initiated de novo. In mammals, the circadian clock located in the suprachiasmatic nuclei (SCN) starts oscillating during late fetal life, and expression of the mouse clock genes *Per1* and *Per2* was observed in the SCN just before or at birth (*4, 9, 25*). However, the discovery of circadian oscillators in peripheral organs and in tissue culture cells indicates that circadian clock function does not necessarily require the completion of long and complex developmental processes such as vertebrate brain development (*10, 17, 26*). In *Drosophila*, *Per* is expressed throughout development, and the onset of circadian behavioral rhythm is light independent; however, its synchronization requires a light-entraining signal (*27*). Our data show that developing zebrafish embryos inherit maternal circadian clock gene products and perhaps also the phase of their clock.

References and Notes

1. C. S. Pittendrigh, *Annu. Rev. Physiol.* **55**, 17 (1993).
2. J. C. Dunlap, *Cell* **96**, 271 (1999).
3. X. Jin *et al.*, *Cell* **96**, 57 (1999).
4. S. M. Reppert, in *Circadian Clocks and Their Adjustment*, vol. 183 of *CIBA Foundation Symposium*, D. J. Chadwick and K. Ackrill, Eds. (Wiley, Chichester, UK, 1995), pp. 198–211.
5. F. Davis and J. Mannion, *Am. J. Physiol.* **255**, R439 (1988).
6. Y. Citri *et al.*, *Nature* **326**, 42 (1987).
7. M. W. Young, *Annu. Rev. Biochem.* **67**, 135 (1998).
8. H. Tei *et al.*, *Nature* **389**, 512 (1997).
9. L. P. Shearman, M. J. Zylka, D. R. Weaver, L. F. Kolakowski Jr., S. M. Reppert, *Neuron* **19**, 1261 (1997).
10. M. J. Zylka, L. P. Shearman, D. R. Weaver, S. M. Reppert, *Neuron* **20**, 1103 (1998).
11. B. Zheng *et al.*, *Nature* **400**, 169 (1999).
12. A zebrafish *Per3* polymerase chain reaction (PCR) probe was amplified with the primers 5′-CTGGG(C/T)TA(C/T)CTICC(C/T)CAGGA-3′ and 5′-CAG(T/C)T(C/G)ATCTGCTG(A/G)TAGGA-3′ and was used for screening a cDNA library of random-primed segmentation-stage zebrafish embryos and a cDNA library of oligo(dT)-primed maternal zebrafish embryos. A full-length and several overlapping independent cDNA clones were obtained and sequenced. The zebrafish *Rev-erbα* (NR1D1) probe was PCR amplified with the primers 5′-GT(T/G)GCITC(G/A)GG(C/A)TT(T/C)CA(C/T)TA-3′ and 5′-GC(A/G)AA(C/T)TC(C/T)ACCACCTC(A/C)CG-3′. The *17βHSD* probe was used as a control (*28*).
13. T. K. Darlington *et al.*, *Science* **280**, 1599 (1998).
14. A. M. Sangoram *et al.*, *Neuron* **21**, 1101 (1998).
15. N. Miyajima *et al.*, *Cell* **57**, 31 (1989).
16. G. Adelmant, A. Bègue, D. Stéhelin, V. Laudet, *Proc. Natl. Acad. Sci. U.S.A.* **93**, 3553 (1996).
17. A. Balsalobre, F. Damiola, U. Schibler, *Cell* **93**, 929 (1998).
18. S. W. Wilson, L. S. Ross, T. Parrett, S. S. Easter Jr., *Development* **108**, 121 (1990).
19. S. W. Wilson and S. S. Easter Jr., *Development* **112**, 723 (1991).
20. F. Delaunay, C. Thisse, O. Marchand, V. Laudet, B. Thisse, data not shown.
21. N. Kazimi and G. M. Cahill, *Dev. Brain Res.* **117**, 47 (1999).
22. Y. Shigeyoshi *et al.*, *Cell* **91**, 1043 (1997).
23. M. Westerfield, *The Zebrafish Book* (Univ. of Oregon Press, Eugene, ed. 3, 1995).
24. D. A. Kane and C. B. Kimmel, *Development* **119**, 447 (1993).
25. M. Seron-Ferré, C. A. Duscay, G. J. Valenzuela, *Endocr. Rev.* **14**, 594 (1993).
26. J. D. Plautz, M. Kaneko, J. C. Hall, S. A. Kay, *Science* **278**, 1632 (1997).
27. A. Sehgal, J. Price, M. W. Young, *Proc. Natl. Acad. Sci. U.S.A.* **89**, 1423 (1992).
28. C. Thisse and B. Thisse, unpublished data.
29. ———, T. F. Schilling, J. H. Postlethwait, *Development* **119**, 1203 (1993).
30. Single-letter abbreviations for the amino acid residues are as follows: A, Ala; C, Cys; D, Asp; E, Glu; F, Phe; G, Gly; H, His; I, Ile; K, Lys; L, Leu; M, Met; N, Asn; P, Pro; Q, Gln; R, Arg; S, Ser; T, Thr; V, Val; W, Trp; and Y, Tyr.
31. The *AB zebrafish strain was kept at 28°C in a LD 14:10 cycle with lights on at 0900 hours (ZT 0). For most experiments, adults were crossed overnight, resulting in spawning and fertilization at about ZT 0, the next morning. Embryos were raised at 28°C in petri dishes containing 0.003% phenylthiourea to prevent pigmentation. Lighting conditions were either LD 14:10, LD 14:10 that was shifted 8 hours forward, LD 8:8, LL, or DD. Delayed development was obtained by keeping embryos at 23°C in LL. For desynchronizing development from the light/dark cycle, adults in LD 14:10 were crossed at ZT 3, and embryos fertilized at ZT 12 the same day were kept in LL. Embryos were fixed for 12 to 16 hours in 4% paraformaldehyde/phosphate–buffered saline at 4-hour intervals and stored in methanol. Unfertilized oocytes were obtained by squeezing mature females under anesthesia at 4-hour intervals.
32. Whole-mount in situ hybridization was performed according to Thisse *et al.* (*29*). Duration of staining was identical for all embryos. In Fig. 3, temporal expression profiles of *Per3* were determined by scoring 10 embryos per point for no, low, medium, or high staining with reference to the respective 40-, 56-, 80-, and 96-hpf time points from Fig. 2. No significant variation of the staining was observed. Reverse transcriptase–PCR (RT-PCR) detection of *Per3* mRNA and *28S* ribosomal RNA (rRNA) was carried out with reverse-transcribed total RNA and the following specific primers: 5′-CGGATCGGTACCTCAGTCCT-3′ and 5′-TCCATTATTATGAACAGGCT-3′ for *Per3* and 5′-CCTCACGATCCTTCTGGCTT-3′ and 5′-AATTCTGCTTCACAATGATA-3′ for *28S* rRNA. The cycle number was optimized for obtaining signals within the linear range. PCR products were analyzed by Southern blot and probed with a specific ^{32}P–end-labeled oligonucleotide.

33. We thank V. Heyer and G. Triqueneaux for technical assistance, O. Nkundwa and A. Karmim for maintenance of zebrafish, J.-M. Vanacker and M. Robinson-Rechavi for critical reading, and B. B. Rudkin for encouragement. This work was supported by funds from the INSERM, the CNRS, the Hôpital Universitaire de Strasbourg, the Association pour la Recherche sur le Cancer, and the Ligue Nationale de Lutte Contre le Cancer. F.D. is the recipient of a long-term postdoctoral fellowship from the Fondation pour la Recherche Médicale.

20 January 2000; accepted 11 May 2000

Requirement of the Spindle Checkpoint for Proper Chromosome Segregation in Budding Yeast Meiosis

Marion A. Shonn,[1]* Robert McCarroll,[2] Andrew W. Murray[1,3]*†

The spindle checkpoint was characterized in meiosis of budding yeast. In the absence of the checkpoint, the frequency of meiosis I missegregation increased with increasing chromosome length, reaching 19% for the longest chromosome. Meiosis I nondisjunction in spindle checkpoint mutants could be prevented by delaying the onset of anaphase. In a recombination-defective mutant (*spo11Δ*), the checkpoint delays the biochemical events of anaphase I, suggesting that chromosomes that are attached to microtubules but are not under tension can activate the spindle checkpoint. Spindle checkpoint mutants reduce the accuracy of chromosome segregation in meiosis I much more than that in meiosis II, suggesting that checkpoint defects may contribute to Down syndrome.

Meiosis I differs from mitosis and meiosis II. In meiosis I, the two sister centromeres remain attached to each other and move to one spindle pole, segregating away from the paired centromeres of the homologous chromosome (Fig. 1A) (*1*). We investigated the meiotic role of the spindle checkpoint, which keeps cells with misaligned chromosomes from starting anaphase by preventing the activation of the anaphase promoting complex (APC, also known as the cyclosome) (*2, 3*). The spindle checkpoint detects kinetochores that are not attached to microtubules (*4, 5*) and the absence of tension at kinetochores that are attached to microtubules (*6*). Mutations in the budding yeast *MAD1*, *MAD2*, *MAD3*, *BUB1*, *BUB3*, and *MPS1* genes eliminate the spindle checkpoint (*7, 8*).

To follow meiotic chromosome segregation, we targeted green fluorescent protein (GFP) to bind a specific chromosome. Tan-

Department of [1]Biochemistry and [3]Department of Physiology, University of California, San Francisco, CA 94143–0444, USA. [2]Cereon Genomics, LLC, 45 Sidney Street, Cambridge, MA 02139, USA.

*Present address: Department of Molecular and Cellular Biology, Harvard University, Cambridge, MA 02138, USA.

†To whom correspondence should be addressed. E-mail: amurray@mcb.harvard.edu

dem repeats of the bacterial lactose operator (LacO) sequence were integrated close to the centromere and seen by binding of a protein fusion between the lactose repressor and GFP (GFP-LacI) (*9, 10*). By marking both homologs of a chromosome, we can determine the pattern of chromosome segregation in meiosis I. If chromosome segregation was normal in both meiotic divisions, all four spores inherit a single copy of the marked locus (Fig. 1A). Meiosis I nondisjunction, the segregation of both homologs to the same spindle pole, produces two spores that lack the marked locus and two spores that have two copies (Fig. 1A).

We analyzed the meiotic segregation of GFP-marked chromosome IV in wild-type and *mad2*Δ cells (Fig. 1B). Chromosome IV nondisjoined in 19% of *mad2*Δ tetrads (Fig. 1C), showing that the spindle checkpoint is required for proper chromosome segregation in meiosis I. The frequency of nondisjunction in meiosis II was statistically indistinguishable between wild-type and *mad2*Δ cells (*11*). In *mad2*Δ diploids, the frequency of nondisjunction in meiosis I increased with increasing chromosome length (Fig. 1C) (*12*). The pattern of spore inviability confirmed that spindle checkpoint mutants suffer from nondisjunction in meiosis I. The *mad1*Δ and *mad2*Δ strains produced an excess of tetrads with two viable and two dead spores. Statistical analysis suggests that nondisjunction events are clustered rather than randomly distributed among all cells (Table 1).

How does the spindle checkpoint improve the fidelity of chromosome segregation in meiosis I? One possibility is that both members of some pairs of homologous chromosomes attach to the same spindle pole and that a checkpoint-dependent delay allows them to reorient and attach to opposite poles (Fig. 1A). This hypothesis predicts that anaphase would occur earlier in *mad2*Δ cells. Using the SK1 background, which gives the best synchrony of sporulation (*13, 14*), we could not detect a change in timing of meiosis I chromosome segregation or spindle breakdown in *mad2*Δ diploids (*15*). However, anaphase begins only 10 min earlier in checkpoint-defective mitotic cells (*16*), a change that we could not detect in the much less synchronous meiotic cell cycle. A second prediction is that imposing a metaphase delay should eliminate meiosis I nondisjunction in spindle checkpoint mutants. Weak expression of a nondegradable form of the anaphase inhibitor Pds1 (*17*) delayed the start of anaphase I and produced two-spored asci (*18*). After the metaphase I delay, the GFP-marked chromosome IV segregated correctly in both wild-type and *mad2*Δ cells (Fig. 1D). Thus, artificially delaying anaphase of meiosis I can prevent nondisjunction in spindle checkpoint mutants. We believe that the formation of two-spored asci in cells expressing nondegradable Pds1 reflects a fixed interval between the formation of a

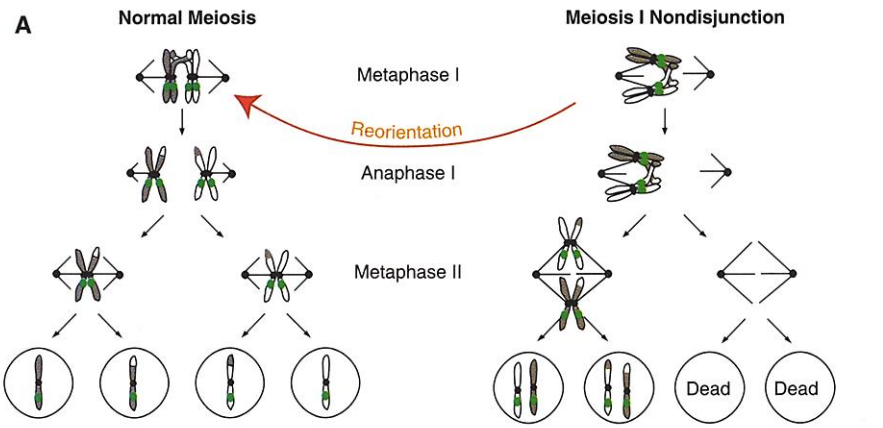

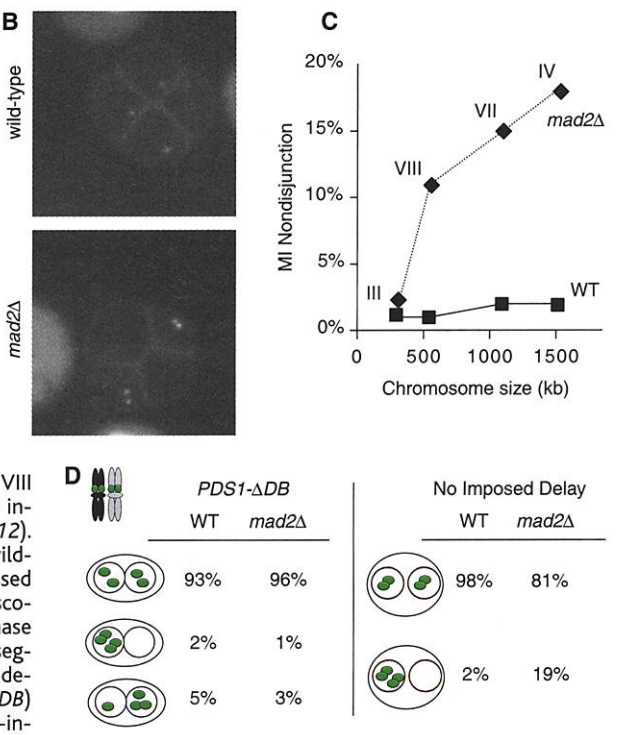

Fig. 1. The spindle checkpoint is required for proper chromosome segregation in meiosis I. (**A**) Chromosome segregation in wild-type cells (left) results in one GFP-marked LacO array (GFP/LacO) in each of four spores that can be detected by fluoresence microscopy. Nondisjunction in meiosis I (right) results in GFP-LacI in two of four spores. (**B**) Chromosome segregation was assessed in tetrads by fluorescence microscopy in wild-type and *mad2*Δ strains that have LacO arrays near the centromere of chromosome IV (*9*). (**C**) Chromosomes III, IV, VII, and VIII were marked with a LacO array integrated near the centromere (*12*). Chromosome segregation in wild-type and *mad2*Δ cells was assessed in tetrads by fluorescence microscopy. MI, meiosis I. (**D**) A metaphase delay rescues the chromosome segregation defect in *mad2*Δ. A nondegradable form of Pds1 (*PDS1-ΔDB*) was expressed from the copper-inducible *CUP1* promoter (*18*). Cells sporulated in 100 μM $CuSO_4$ arrest with a single short spindle. Cells sporulated in 5 μM $CuSO_4$ accumulated short spindles, but completed a single meiotic division in which the segregation efficiency of chromosome IV was similar in wild type (WT) and *mad2*Δ. In the absence of copper, cells continued through a second division to form tetrads. Nondisjunction frequency in the absence of copper was determined in tetrads.

Table 1. Spore viability in spindle checkpoint mutants. Distribution of spore viability in wild-type (WT), *mad1*Δ, and *mad2*Δ tetrads. Viability was assessed by dissecting tetrads. If nondisjunction events are not clustered, we can use the Poisson distribution and the frequency of tetrads with four viable spores to calculate the mean number of nondisjunction events per cell as 0.844. Another value of the same parameter, 1.35, was derived using the cytologically measured nondisjunction frequencies for several chromosomes (Fig. 1C). The fraction of four-spored tetrads predicted using this average nondisjunction frequency is significantly different from that observed (χ^2 test, $P < 0.01$). Bold values differ markedly from those for the wild type.

Strain	Ratio of live:dead spores					Percent viability of spores
	4:0	3:1	2:2	1:3	0:4	
WT	94%	3%	3%	0%	0%	98% (n = 304)
*mad2*Δ	43%	8%	**26%**	2%	**22%**	62% (n = 420)
*mad1*Δ	42%	4%	**24%**	2%	**28%**	58% (n = 100)

meiosis I spindle and spore formation. If anaphase of meiosis I is sufficiently delayed, spores will form before meiosis II occurs.

In mitosis, the spindle checkpoint arrests cells that lack a mitotic spindle. Does this checkpoint have a similar function in meiosis? We incubated wild-type cells in sporulation medium containing the microtubule poison benomyl (*19*). The cells arrested with a single mass of DNA and two closely spaced spindle pole bodies (Fig. 2, A and C). In contrast, benomyl-treated, checkpoint-deficient *mad2*Δ cells completed two meiotic divisions (Fig. 2B), although they suffered massive missegregation in both meiosis I and meiosis II (*15*).

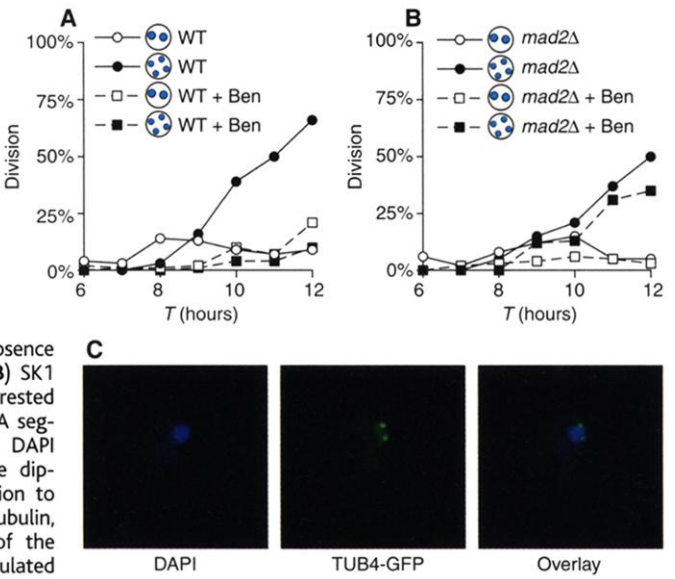

Fig. 2. Kinetochore attachment sensed by the meiotic spindle checkpoint. (**A**) Wild-type SK1 diploids were induced to undergo a synchronous meiosis (*13*), and DNA segregation was assayed by DAPI (4′,6′-diamidino-2-phenylindole) staining. Lines show cells with two (open symbols) and four (closed symbols) DNA masses in the presence or absence of benomyl as indicated. (**B**) SK1 *mad2*Δ diploids were not arrested by 60 μg/ml benomyl. DNA segregation was assessed by DAPI staining. (**C**) SK1 wild-type diploids expressing a GFP fusion to *TUB4*, the yeast gamma tubulin, which acts as a marker of the spindle pole body were sporulated in the presence of benomyl (*42*).

We investigated how the linkage between homologous chromosomes regulates the spindle checkpoint. This linkage is created by reciprocal recombination and causes tension on the kinetochore-microtubule connections as they pull against each other. Tension is thought to signal to the checkpoint that the homologs are attached to opposite poles (*6*). The *spo11*Δ mutant completely abolishes meiotic recombination, preventing linkage of homologous chromosomes (*20*) and causing random segregation of GFP-marked homologs at meiosis I (*15, 21*). In insect spermatocytes, the absence of tension at the kinetochore can activate the spindle checkpoint in meiosis (*6*). However, because animal kinetochores have many microtubule binding sites, the effect of tension could be indirect, causing some sites to lose their microtubules and thus activate the checkpoint. In contrast, yeast kinetochores are captured by a single microtubule in mitotic cells (*22*), and data from meiotic spindles suggests that single microtubules attach to kinetochores in meiotic divisions as well (*23*). The absence of a mechanical link between homologs (*spo11*Δ) does not appear to affect microtubule attachment of a GFP-marked homolog in meiosis I (*24*), suggesting that experiments in yeast directly measure the effects of tension, as opposed to effects of destabilizing the link between kinetochores and microtubules.

The kinetochores of linked homologs pull against each other, thus preventing spindle elongation until the linkage dissolves (*25, 26*). To follow the state of the cell cycle machinery, we examined the destruction of Pds1 as a biochemical marker for the start of anaphase. In wild-type meiosis I, Pds1 behaved exactly as it does in mitosis: it was present in cells with a single short spindle (metaphase I) and absent from cells with a long spindle and two separated DNA masses (anaphase I), showing that the APC had been activated (Fig. 3A). Although DNA staining suggested that *spo11*Δ cells had completed anaphase of meiosis I, spindle elongation had occurred before the biochemical events that trigger chromosome separation: Pds1 was present in 77% of the *spo11*Δ cells with a long spindle connecting two DNA masses (Fig. 3A). If *spo11*Δ cells cannot maintain a short metaphase I spindle because their homologs are not linked, there should be fewer short spindles in a *spo11*Δ strain. Only 5% of *spo11*Δ cells have short spindles compared to 20% of wild-type cells (*15*),

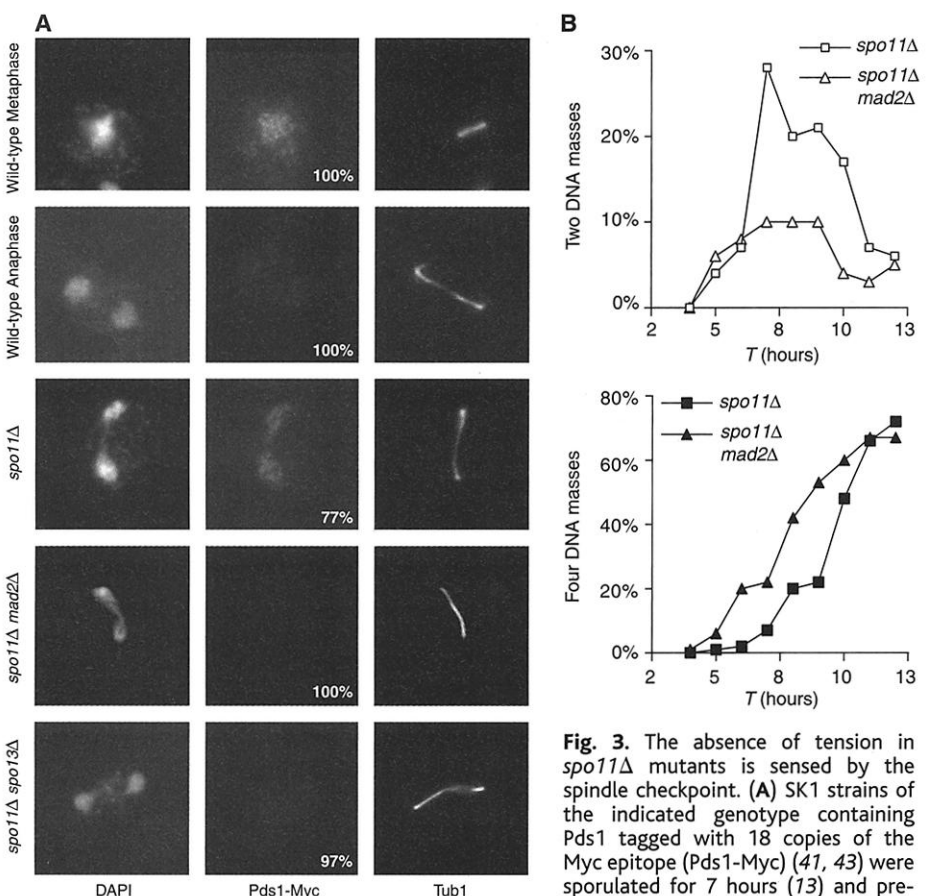

Fig. 3. The absence of tension in *spo11*Δ mutants is sensed by the spindle checkpoint. (**A**) SK1 strains of the indicated genotype containing Pds1 tagged with 18 copies of the Myc epitope (Pds1-Myc) (*41, 43*) were sporulated for 7 hours (*13*) and prepared for indirect immunofluorescence against tubulin (Tub1) and the Myc epitope; DNA was stained with DAPI (*44*). (**B**) DNA segregation in *spo11*Δ and *spo11*Δ *mad2*Δ during sporulation (*13*), as assayed by DAPI staining. At least 200 cells were scored for each time point.

demonstrating that without a mechanical link between homologous chromosomes, the meiosis I spindle elongates even though the APC has not been activated, as do spindles in mitotic cells with unlinked sister chromatids (*27, 28*).

If the spindle checkpoint senses kinetochore tension, checkpoint components should be required to stabilize Pds1 in *spo11*Δ mutants. Pds1 had been destroyed in every *spo11*Δ *mad2*Δ cell that produced two DNA masses on a long meiosis I spindle, indicating that APC activation had occurred at the same time as spindle elongation (Fig. 3A). Furthermore, in *spo11*Δ mutants with an intact checkpoint, there were more cells with two DNA masses (suggesting a delay in completing meiosis I) (*29*), and the completion of meiosis II was delayed by about 1 hour compared to *spo11*Δ *mad2*Δ cells (Fig. 3B). Because chromosome attachment appeared unaffected in *spo11*Δ cells, these data suggest that the spindle checkpoint can detect a lack of tension in meiosis I and delay Pds1 destruction and meiotic progression. The absence of Spo11 has been reported to affect the timing of the meiotic cell cycle, advancing both DNA replication (*30*) and the completion of meiosis I (*29*). The latter claim reflects the interpretation that cells with two DNA masses have activated the APC and reveals the danger of using the distribution of DNA in mutant cells to imply the stage of the cell cycle.

Does spindle elongation in *spo11*Δ cells reflect the absence of a connection between homologs? We restored centromere linkage to *spo11*Δ mutants by removing Spo13, a protein required to prevent sister kinetochores from separating at anaphase of meiosis I. In the *spo11*Δ *spo13*Δ double mutant, a single mitosis-like division occurs: the sister chromatids of the unrecombined chromosomes attach to and segregate to opposite poles (*31*). In the double mutant, 50% of the meiosis I spindles were short, indicating that sister kinetochores prevent the spindle from elongating (*15*), and long spindles were only seen in cells that lacked Pds1 (Fig. 3A). Thus, restoring the bipolar attachment of kinetochores made spindle elongation and chromosome segregation depend on APC activation.

We have shown that the budding yeast spindle checkpoint, which is largely dispensable in wild-type mitosis (*7*), plays a critical role in meiotic chromosome segregation. This difference may reflect the different chromosome linkages in mitosis and meiosis I. In mitosis, sister chromatid cohesion forces sister kinetochores to face opposite spindle poles. In meiosis I, homologs are linked at sites of recombination that can be far from the kinetochores, creating a floppy linkage (*32–34*). If the nearest recombination event is further from the centromere on long chromosomes, this idea may explain why long chromosomes preferentially nondisjoin in checkpoint-defective cells.

Our findings may be relevant to Down syndrome. This birth defect is mostly caused by nondisjunction of chromosome 21 in meiosis I and is correlated with increased maternal age and chromosomes whose recombination events are far from the centromere (*35*). These chromosomes apparently nondisjoin more often in older mothers because of age-dependent loss of a factor required for accurate segregation (*36, 37*). Our findings suggest that the spindle checkpoint is a candidate for this factor.

References and Notes

1. G. S. Roeder, *Genes Dev.* **11**, 2600 (1997).
2. S. H. Kim, D. P. Lin, S. Matsumoto, A. Kitazono, T. Matsumoto, *Science* **279**, 1045 (1998).
3. L. H. Hwang *et al.*, *Science* **279**, 1041 (1998).
4. C. L. Rieder, A. Schultz, R. Cole, G. Sluder, *J. Cell Biol.* **127**, 1301 (1994).
5. J. C. Waters, R. H. Chen, A. W. Murray, E. D. Salmon, *J. Cell Biol.* **141**, 1181 (1998).
6. X. Li and R. B. Nicklas, *Nature* **373**, 630 (1995).
7. R. Li and A. W. Murray, *Cell* **66**, 519 (1991).
8. M. A. Hoyt, L. Trotis, B. T. Roberts, *Cell* **66**, 507 (1991).
9. A. F. Straight, A. S. Belmont, C. C. Robinett, A. W. Murray, *Curr. Biol.* **6**, 1599 (1996).
10. GFP-LacI expression driven by *CYC1* promoter, pAFS 152 (*38*).
11. If only one homolog is marked with GFP, normal segregation of the two sister chromatids in meiosis II will produce two spores that have a single copy of the GFP-marked chromosomes. Nondisjunction in meiosis II will lead to a single spore that contains two copies of the GFP marked chromosome. The measured frequencies of nondisjunction in wild-type strains are higher than those reported from genetic tests (*39*). We believe that this discrepancy is due to a low frequency of recombination events that reduce the number of Lac operator repeats below the threshold required for detection.
12. All strains are in the W303 background, unless otherwise noted: *MAT a/MATα, ura3-1 leu2, 3-112, his3-11, trp1-1, ade2-1, can1-100*. All mutations are homozygous unless otherwise noted. GFP tagging of chromosome IV (MAS 386, 327; wild-type and *mad2*Δ, respectively) and III (MAS 401, 424) is described in (*9*). Strains MAS 559, 561 were constructed by integrating pMAS72 near the centromere of chromosome VII. Plasmid pMAS72 contains a Bam HI–Sac I fragment spanning nucleotides 478360 through 479162 of chromosome VII in plasmid pAFS149 (*38*) which contains 128 repeats of LacO. Strains MAS 656, 658 were constructed by integrating pMAS79 near the centromere of chromosome VIII. Plasmid pMAS79 contains a Bam HI–Sac I fragment spanning nucleotides 123761 through 124110 on chromosome VIII in pAFS149. All experiments were repeated at least twice with similar results. In all experiments, at least 200 cells were counted.
13. We used the SK1 strain background for all experiments requiring a rapid, synchronous meiosis. Synchronous sporulation in 2% potassium acetate as in (*14*). All SK1 strains derived from NKY 611: *leu2::hisG ura3, ho::LYS2, lys2*. SK1 wild-type: MAS 120, SK1 *mad2*Δ: MAS 403. SK1 *mad2*Δ mutants also undergo meiosis I nondisjunction, but at higher levels than W303.
14. R. Padmore, L. Cao, N. Kleckner, *Cell* **66**, 1239 (1991).
15. M. A. Shonn, R. McCarroll, A. W. Murray, data not shown.
16. S. Biggins, A. Rudner, A. Murray, unpublished data.
17. O. Cohen-Fix, J. M. Peters, M. W. Kirschner, D. Koshland, *Genes Dev.* **10**, 3081 (1996).
18. *pCUP1-PDS1-DB*Δ (pMAS74) was integrated into wild-type (MAS 612) and *mad2*Δ (MAS 611) strains that have chromosome IV marked with GFP and sporulated in the presence of 0, 5, or 100 μM copper sulfate. Plasmid pMAS74 was constructed by ligating a SalI/PstI fragment of pRTK-C2 (*40*) into pBS156 (B. Stern, unpublished data) which contains a fragment of the *CUP1* promoter. Cells sporulated in 5 μM $CuSO_4$ formed dyads at reduced efficiency compared to those sporulated in the absence of copper. Sister chromatid separation occurs in only 4% of divisions for both wild type and *mad2*Δ.
19. SK1 cells were sporulated for 4 hours at room temperature in 2% potassium acetate as in (*13*), then resuspended in 2% potassium acetate plus 60 μg/ml benomyl, prepared by adding a 30 mg/ml stock of benomyl in dimethyl sulfoxide to boiling media and slowly cooling to room temperature. Cells were fixed in 40% ethanol and 0.1 M sorbitol.
20. L. Cao, E. Alani, N. Kleckner, *Cell* **61**, 1089 (1990).
21. F. Klein *et al.*, *Cell* **98**, 91 (1999).
22. M. Winey *et al.*, *J. Cell Biol.* **129**, 1601 (1995).
23. G. Morgan, T. H. Giddings Jr., P. D. Straight, M. Winey, personal communication.
24. We determined the position of chromosome III homologs on the long meiosis I spindle in *spo11*Δ (SK1 strain MAS 645: LacO:*LEU2* GFP-LacI *spo11*Δ) by indirect immunofluorescence against Tub1 and GFP-LacI. We find that the marked centromere is always pulled to a spindle pole, suggesting that homologs are attached to the spindle.
25. J. C. Waters, R. V. Skibbens, E. D. Salmon, *J. Cell Sci.* **109**, 2823 (1996).
26. C. Michaelis, R. Ciosk, K. Nasmyth, *Cell* **91**, 35 (1997).
27. S. Piatti, C. Lengauer, K. Nasmyth, *EMBO J.* **14**, 3788 (1995).
28. B. Stern and A. Murray, unpublished data.
29. A. M. Galbraith, S. A. Bullard, K. Jiao, J. J. Nau, R. E. Malone, *Genetics* **146**, 481 (1997).
30. R. Cha, B. Weiner, S. Keeney, J. Dekker, N. Kleckner, *Genes Dev.* **14**, 493 (2000).
31. S. Klapholz and R. E. Esposito, *Genetics* **96**, 589 (1980).
32. R. B. Nicklas, *Genetics* **78**, 205 (1974).
33. L. O. Ross, R. Maxfield, D. Dawson, *Proc. Natl. Acad. Sci. U.S.A.* **93**, 4979 (1996).
34. K. E. Koehler *et al.*, *Nature Genet.* **14**, 406 (1996).
35. S. L. Sherman *et al.*, *Hum. Mol. Genet.* **3**, 1529 (1994).
36. N. E. Lamb *et al.*, *Nature Genet.* **14**, 400 (1996).
37. R. S. Hawley, J. A. Frazier, R. Rasooly, *Hum. Mol. Genet.* **3**, 1521 (1994).
38. A. Straight, unpublished data.
39. S. Sora, G. Lucchini, G. Magni, *Genetics* **101**, 17 (1982).
40. R. L. Tinker-Kulberg and D. O. Morgan, *Genes Dev.* **13**, 1936 (1999).
41. M. Shirayama, W. Zachariae, R. Ciosk, K. Nasmyth, *EMBO J.* **17**, 1336 (1998).
42. Plasmid pMAS68 was constructed by inserting a fragment of the *TUB1* promoter into pAFS160 (*38*) which contains a fusion between TUB4 and GFP. Plasmid was integrated at *URA3* to create SK1 strain MAS 601.
43. SK1 wild-type (MAS608), *spo11*Δ (MAS613), *spo11*Δ *mad2*Δ (MAS613), and *spo11*Δ *spo13*Δ (MAS 659) homozygous diploids all express the Pds1 protein tagged with 18 copies of the Myc epitope (*41*).
44. M. Rose, F. Winston, P. Heiter, *Methods in Yeast Genetics* (Cold Spring Harbor Press, Cold Spring Harbor, NY, 1990).

45. We thank M. Winey for sharing unpublished information and S. Roeder, S. Hawley, B. Nicklas, and members of the Murray lab for critical reading of the manuscript. We are grateful to the Kleckner lab for SK1 strains. Supported by grants from NIH and the Human Frontiers In Science Program.

28 March 2000; accepted 3 May 2000